DOI: 10.1002/chem.201103078

Flexible Metal–Organic Framework with Hydrophobic Pores

Lin-Hua Xie and Myunghyun Paik Suh*[a]

In recent years, metal–organic frameworks (MOFs)[1] have been intensively studied due to their potential to be applied in gas storage and separation,[2] chemical sensors,[3] catalysis,[4] fabrication of metal nanoparticles,[5] etc. Many advantages of MOFs, including flexibility and designability have motivated researchers to explore smarter materials in many areas. In most practical application processes, effects of surrounding water molecules on the MOF materials have to be considered. For example, in gas storage and separation, MOFs can be degraded or their pores can be preoccupied by water molecules contained in the relevant gases.[6] Also, in catalysis, MOF catalysts are easily poisoned by water molecules from air or those produced by the organic reactions being catalyzed.[7] It is highly desirable to develop porous materials that are immune to the negative effects of water. The demand has inspired research interest in introducing hydrophobicity to MOFs.[8]

Here we present a new MOF, $[Cu_4(Me_3CCOO)_8(teia)]$ (teia = 1,3,5,7-tetrakis(4-(2-ethyl-1*H*-imidazol-1-yl)phenyl)-adamantane) (**SNU-80**), which excludes water molecules even under saturated water vapour pressure at room temperature, although its pores are large enough for most common gases to diffuse into. **SNU-80** is flexible with alterable pores as well, which leads to stepwise adsorption of N_2, O_2, and CO_2 gases. We also demonstrate for the first time that the structural flexibility of a MOF profoundly enhances its hydrophobicity and stability against water on removal of guest molecules.

Green crystals of the as-synthesized phase of **SNU-80**, $[Cu_4(Me_3CCOO)_8(teia)]\cdot 7.5\,PrOH$ (**SNU-80a**), were prepared by the reaction of copper pivalate and the tetrahedral shaped ligand teia in PrOH at room temperature (Figure 1). Single-crystal X-ray diffraction study of **SNU-80a** reveals that each teia coordinates four Cu^{2+} ions of four $[Cu_2(Me_3CCOO)_4]$ paddle-wheel units through the terminal N atoms, and every $[Cu_2(Me_3CCOO)_4]$ unit binds two teia ligands at the apical sites of the Cu^{2+} ions (Figure 2a).[9] The connectivity of the teia ligands and the paddle-wheel units leads to a distorted diamondoid network, and six such diamondoid networks are interpenetrated (Figure 2b). It is worth noting that the copper paddle-wheel cluster serves as linear linker here, while copper paddle-wheel clusters commonly act as topological square-planar nodes in carboxylate-based MOFs such as HKUST-1.[10] There exist one-dimensional channels with a diameter of about 6.5–7.0 Å along the *c* axis (Figure 2c). The channels are occupied by disordered guest molecules. The solvent-accessible volume is 44% of the whole structure as estimated by PLATON.[11] The theoretical surface area of the framework of **SNU-80a** is 1440 $m^2 g^{-1}$ as estimated with Materials Studio Program.[12] Thermogravimetric (TG) curve and elemental analysis (EA) data indicate that **SNU-80a** includes 7.5 PrOH as guests per formula unit of the host framework (see the Supporting Information). The channel surfaces are lined with the hydrophobic *tert*-butyl groups of pivalate anions and ethyl groups of teia ligands.

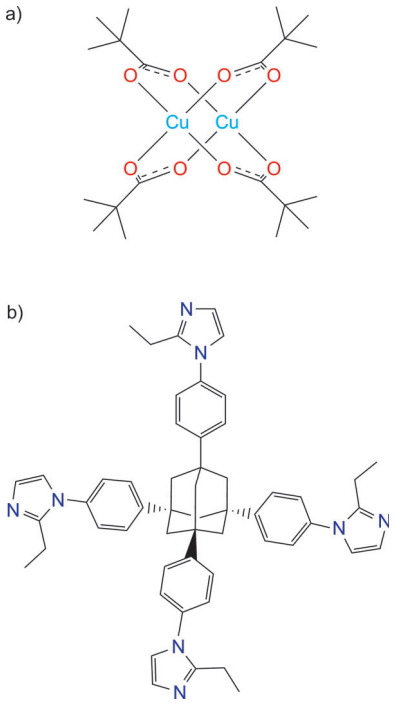

Figure 1. Molecular building blocks of **SNU-80a**. a) Paddle-wheel shaped copper pivalate dimer, b) tetrahedral shaped ligand teia.

The guest molecules in **SNU-80a** were completely removed by treatment with supercritical CO_2, as confirmed by EA and TG curves, which resulted in **SNU-80**. The powder

[a] Dr. L.-H. Xie, Prof. M. P. Suh
Department of Chemistry, Seoul National University
Seoul 151-747 (Republic of Korea)
Fax: (+82) 2-886-8516
E-mail: mpsuh@snu.ac.kr

Supporting information for this article is available on the WWW under http://dx.doi.org/10.1002/chem.201103078.

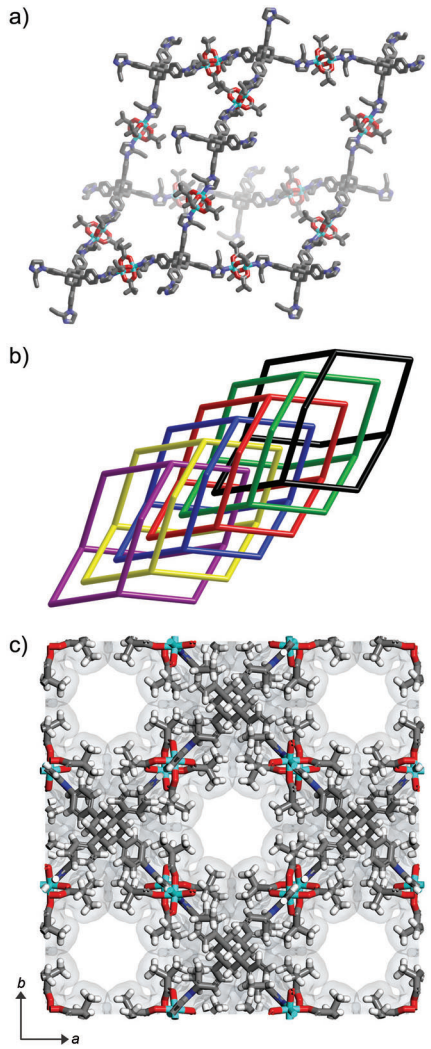

Figure 2. The X-ray crystal structure of **SNU-80a**. a) A diamondoid network formed by connectivity of teia ligands and paddle-wheel shaped $[Cu_2(Me_3CCOO)_4]$ units; for clarity, hydrogen atoms are not shown. b) A simplified representation of sixfold interpenetrated diamondoid networks. c) A perspective view showing the channels extending along the *c* axis formed by the sixfold interpenetrated networks. Cu: turquoise, C: grey, H: white, N: blue, O: red.

X-ray diffraction (PXRD) patterns showed that the framework structure was altered upon removal of guest molecules (Figure S4 in the Supporting Information). The main PXRD peaks of **SNU-80** shifted to higher 2θ angles compared with those of **SNU-80a**, indicating shrinkage of the framework. Indexing and Pawley refinement of the PXRD data for **SNU-80** revealed that the structure transformed from tetragonal into triclinic (see the Supporting Information). When **SNU-80a** was activated at 40 or 100 °C under vacuum, the crystallinity of the sample became much poorer than that activated by supercritical CO_2 (Figure S4 in the Supporting Information). The supercritical CO_2 treatment must be a better activation method in the present case, as demonstrated previously with other MOFs.[13]

To evaluate the porosity of **SNU-80**, gas sorption studies were performed for N_2, O_2, CO_2, H_2, CH_4, and H_2O. The results are summarized in Table S2 in the Supporting Information. In the N_2 adsorption isotherm at 77 K, a two-step adsorption process with a profound desorption hysteresis was observed (Figure 3). The first step of the adsorption curve,

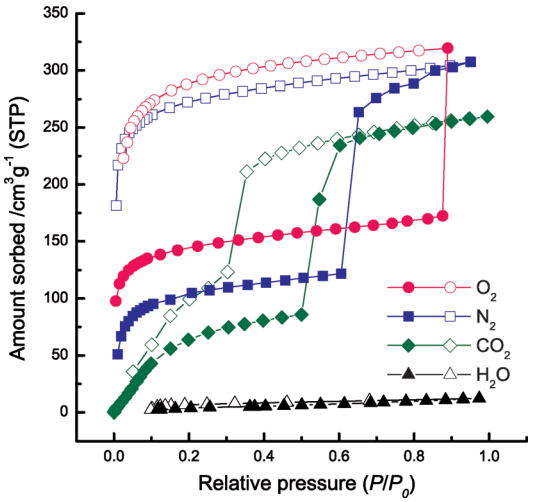

Figure 3. Adsorption isotherms for N_2 (77 K), O_2 (77 K), CO_2 (195 K), and H_2O (298 K). Filled shapes: adsorption; open shapes: desorption; P/P_0 is the ratio of gas pressure (P) to saturation pressure (P_0); P_0 equals 760 Torr for N_2 at 77 K and for CO_2 at 195 K, 155.73 Torr for O_2 at 77 K, and 23.57 Torr for H_2O at 298 K.

in the range of $P/P_0 = 0.01$–0.61, resembles a typical type-I isotherm that is characteristic for a microporous material. At higher pressures ($P/P_0 > 0.61$), the second step of the adsorption occurs. The desorption curve does not retrace the adsorption curve, and the amount of adsorbed N_2 decreases slowly until the pressure approaches $P/P_0 = 0.1$. Two successive N_2 adsorption measurements revealed that the isotherm with the two-step adsorption and hysteretic desorption was reproducible (Figure S6 in the Supporting Information). As mentioned earlier, PXRD patterns show that the structure shrinks after activation of **SNU-80a** to **SNU-80**; this indicates the presence of bistable states of the framework, which must be related with the two-step adsorption isotherm of **SNU-80**.

The first step of N_2 adsorption should be related with the structure of **SNU-80** with shrunken pores, and the structure expands above the gate-opening pressure (P_{go}, $P/P_0 = 0.61$) to provide the second step adsorption. From the adsorption data in the range of $P/P_0 = 0.01$–0.1, the apparent Langmuir and BET surface areas of the shrunken-pore phase of **SNU-80** were estimated to be 456 and 398 $m^2 g^{-1}$, respectively, and the pore volume estimated by the Dubinin–Radushkevich (DR) equation was 0.18 $cm^3 g^{-1}$. It is evident that the expanded-pore phase does not change back to the shrunken-pore phase of **SNU-80** during the desorption process, since the uptake amounts of N_2 gas in the whole desorption curve

are much higher than that at the P_{go} point. Consequently, the data from the desorption curve can be suitable for characterizing the expanded-pore phase. Apparent Langmuir, BET surface areas, and pore volume for the expanded-pore phase estimated by the desorption data in $P/P_0 = 0.01$–0.1 range are 1167 $m^2 g^{-1}$, 1035 $m^2 g^{-1}$, and 0.43 $cm^3 g^{-1}$, respectively, almost 2.5-times higher than those of shrunken phase. Similar to the present case, it was previously demonstrated for other MOFs that the multistep adsorption behaviours were related with the structural transformations during the gas adsorption processes.[2c,14]

As shown in Figure 3, the O_2 (77 K) and CO_2 (195 K) gas adsorption measurements for **SNU-80** also produced well-defined two-step isotherms. High-pressure CO_2 adsorption isotherms measured at 298 K also exhibited a two-step characteristic with a hysteretic desorption curve (Figure S7 in the Supporting Information).

The H_2 adsorption isotherms were measured at 77 and 87 K. The H_2 uptake capacities of **SNU-80** are 0.53 and 0.36 wt%, respectively, under 1 atm (Figure S8 in the Supporting Information). Virial analysis of these isotherms reveals that the isosteric heat (Q_{st}) of the H_2 adsorption at zero surface coverage is 7.19 kJ mol^{-1}, which decreases as the amount of H_2 loading increases (Figure S10 in the Supporting Information). This Q_{st} value is higher than those of MOF-5 (5.2 kJ mol^{-1}) and HKUST-1 (6.6 kJ mol^{-1}),[15] and it can be attributed to overlap of potential energy fields in the narrow pore walls of **SNU-80**.

The CH_4 adsorption isotherm recorded at 195 K shows an uptake of 38 $cm^3 g^{-1}$ at 1 atm (Figure S8 in the Supporting Information). The moderate uptake of CH_4 reveals that the pore size of **SNU-80** is still larger than the kinetic diameter of CH_4 (3.80 Å), even though the framework of **SNU-80** has shrunken from **SNU-80a**.

Water vapour adsorption experiments were conducted at 298 K. Interestingly, **SNU-80** adsorbed only 12 $cm^3 g^{-1}$ (0.55 mol, 0.98 wt%) of water vapour at $P/P_0 = 0.97$ (Figure 3). To confirm the result, a sample of **SNU-80** was kept under the saturated water vapour pressure at room temperature for one week. The TG curve of the moisture-exposed sample showed 1.0% weight loss at 25–150 °C (Figure S11 in the Supporting Information). Its EA data (C: 59.34%; H, 6.81%; N, 5.88%) were very similar to those of the freshly prepared **SNU-80** (C, 59.67%; H, 7.04%; N, 5.97%). The PXRD patterns of **SNU-80** revealed that the framework structure was unchanged after exposure to saturated water vapour at room temperature for one week as well as after immersion in liquid water for one week (Figure S4 in the Supporting Information). In contrast, on exposure to PrOH vapour for 2 h, the framework structure of **SNU-80** was restored to that of **SNU-80a**, as indicated by PXRD patterns (Figure S4 in the Supporting Information). The results demonstrate that the pores of **SNU-80** are highly hydrophobic, despite the fact that the pore sizes are larger than the kinetic diameter of water molecules (2.65 Å), as evidenced by the adsorption of CH_4 gas (kinetic diameter, 3.80 Å).

A small amount of water adsorption is believed to occur at defective outer surfaces of microcrystalline samples.[16] It is common that hydrophobic adsorbents essentially show no uptake of water molecules under low water vapour pressures ($P/P_0 < 0.4$), but most of them exhibit water uptakes at higher water vapour pressures followed by water capillary condensation.[8d,17] No essential water uptake even at saturated water vapour pressure by **SNU-80** can be attributed to its narrow channel size (3.8–6.5 Å), and water molecules cannot be stabilized by interaction with neighbouring water molecules inside the pores. Indeed, it has been revealed previously by single-crystal X-ray analysis of peptide structures that water wires form inside hydrophobic channels of approximately 7.5 Å in size, whereas no water is present in hydrophobic channels of about 5.2 Å.[18] Simulation studies by Coudert et al. also showed that water condensation was shifted to higher water vapour pressures when the pore size of Al(OH)(1,4-NDC) was reduced by methylation of the naphthalene aromatic rings.[19]

In contrast to desolvated **SNU-80**, which was stable in saturated water vapour as well as in liquid water, the green crystals of as-synthesized **SNU-80a** became amorphous after being immersed in water for 6 h (Figure S12 in the Supporting Information), and degraded to colourless powder after being immersed in water for 2 days, which was ascribed to the ligand teia by NMR spectroscopy. For a better understanding of this process, we conducted Grand Canonical Monte Carlo (GCMC) simulations for water adsorption in the framework of **SNU-80a** (see the Supporting Information).[12] The results indicate that at low pressures, water molecules are adsorbed around some corner sites that are formed by imidazole rings and neighbouring paddle-wheel units (Figure 4), suggesting that the pore surfaces at these corner sites are hydrophilic. At high pressures, additional water molecules are adsorbed to the vicinity of the previously adsorbed water molecules (Figure S13 in the Supporting Information). One can also obtain similar results by careful inspection of charge distribution of the framework atoms in

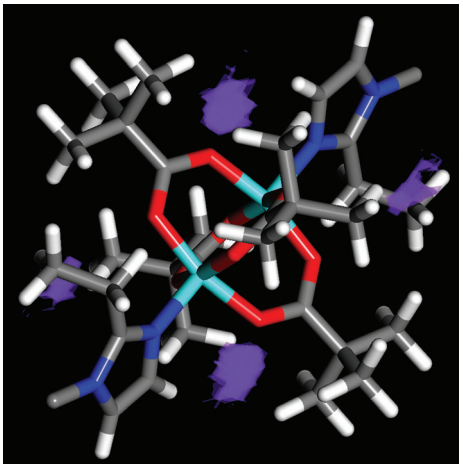

Figure 4. Initial water adsorption sites of the framework of **SNU-80a** obtained from GCMC simulations, which are represented by violet areas.

SNU-80a as calculated by density functional theory. Surfaces of highly charged atoms are well covered by nearly nonpolar *tert*-butyl groups, except the areas of the above-mentioned hydrophilic sites (Figures S14 and S15 in the Supporting Information). These hydrophilic sites are not only the initial water adsorption sites but also the places where water molecules start to attack the framework. On the other hand, the strong hydrophobicity of **SNU-80** implies that structural transformation from **SNU-80a** to **SNU-80** significantly changes the pore surface. After the rearrangement, the sixfold interpenetrated networks shrink and provide reduced pores, then the pore surface must be lined with more crowded *tert*-butyl and ethyl groups, and previous hydrophilic sites no longer exist on the pore surface.

In summary, we have synthesized a new MOF, which adsorbs most common gases, but does not adsorb water molecules even under saturated water vapour pressure at room temperature. The high hydrophobicity of its pore surface benefits from the structural shrinkage of its as-synthesized phase upon guest removal. The framework is also able to transform its structure in response to adsorption of O_2, N_2, and CO_2 to exhibit stepwise adsorption isotherms.

Acknowledgements

This work was supported by a National Research Foundation of Korea (NRF) grant funded by the Korean Government (MEST; Nos.: 2010-0029651 and 2011-001341).

Keywords: flexible networks · gas sorption · hydrophobic effect · metal–organic frameworks · stepwise adsorption

[1] a) O. M. Yaghi, M. O'Keeffe, N. W. Ockwig, H. K. Chae, M. Eddaoudi, J. Kim, *Nature* **2003**, *423*, 705–714; b) S. Kitagawa, R. Kitaura, S. Noro, *Angew. Chem.* **2004**, *116*, 2388–2430; *Angew. Chem. Int. Ed.* **2004**, *43*, 2334–2375; c) G. Férey, *Chem. Soc. Rev.* **2008**, *37*, 191–214; d) J. R. Long, O. M. Yaghi, *Chem. Soc. Rev.* **2009**, *38*, 1213–1214.

[2] a) Y. G. Lee, H. R. Moon, Y. E. Cheon, M. P. Suh, *Angew. Chem.* **2008**, *120*, 7855–7859; *Angew. Chem. Int. Ed.* **2008**, *47*, 7741–7745; b) Y. E. Cheon, M. P. Suh, *Angew. Chem.* **2009**, *121*, 2943–2947; *Angew. Chem. Int. Ed.* **2009**, *48*, 2899–2903; c) H.-S. Choi, M. P. Suh, *Angew. Chem.* **2009**, *121*, 6997–7001; *Angew. Chem. Int. Ed.* **2009**, *48*, 6865–6869; d) Z. R. Herm, J. A. Swisher, B. Smit, R. Krishna, J. R. Long, *J. Am. Chem. Soc.* **2011**, *133*, 5664–5667.

[3] a) Y. Takashima, V. M. Martínez, S. Furukawa, M. Kondo, S. Shimomura, H. Uehara, M. Nakahama, K. Sugimoto, S. Kitagawa, *Nat. Commun.* **2011**, *2*, 168; b) Z.-Z. Lu, R. Zhang, Y.-Z. Li, Z.-J. Guo, H.-G. Zheng, *J. Am. Chem. Soc.* **2011**, *133*, 4172–4174.

[4] a) C.-D. Wu, W. Lin, *Angew. Chem.* **2007**, *119*, 1093–1096; *Angew. Chem. Int. Ed.* **2007**, *46*, 1075–1078; b) O. K. Farha, A. M. Shultz, A. A. Sarjeant, S. T. Nguyen, J. T. Hupp, *J. Am. Chem. Soc.* **2011**, *133*, 5652–5655.

[5] a) H. R. Moon, J. H. Kim, M. P. Suh, *Angew. Chem.* **2005**, *117*, 1287–1291; *Angew. Chem. Int. Ed.* **2005**, *44*, 1261–1265; b) M. P. Suh, H. R. Moon, E. Y. Lee, S. Y. Jang, *J. Am. Chem. Soc.* **2006**, *128*, 4710–4718; c) Y. E. Cheon, M. P. Suh, *Chem. Eur. J.* **2008**, *14*, 3961–3967.

[6] a) J. J. Low, A. I. Benin, P. Jakubczak, J. F. Abrahamian, S. A. Faheem, R. R. Willis, *J. Am. Chem. Soc.* **2009**, *131*, 15834–15842; b) S. Keskin, T. M. van Heest, D. S. Sholl, *ChemSusChem* **2010**, *3*, 879–891.

[7] J. Canivet, S. Aguado, C. Daniel, D. Farrusseng, *ChemCatChem* **2011**, *3*, 675–678.

[8] a) J. G. Nguyen, S. M. Cohen, *J. Am. Chem. Soc.* **2010**, *132*, 4560–4561; b) T. Wu, L. Shen, M. Luebbers, C. Hu, Q. Chen, Z. Ni, R. I. Masel, *Chem. Commun.* **2010**, *46*, 6120–6122; c) D. Ma, Y. Li, Z. Li, *Chem. Commun.* **2011**, *47*, 7377–7379; d) C. Montoro, F. t. Linares, E. Quartapelle Procopio, I. Senkovska, S. Kaskel, S. Galli, N. Masciocchi, E. Barea, J. A. R. Navarro, *J. Am. Chem. Soc.* **2011**, *133*, 11888–11891; e) L. Pan, B. Parker, X. Huang, D. H. Olson, Lee, J. Li, *J. Am. Chem. Soc.* **2006**, *128*, 4180–4181; f) L. Hou, Y. Y. Lin, X. M. Chen, *Inorg. Chem.* **2008**, *47*, 1346–1351; g) S. Q. Ma, D. F. Sun, D. Q. Yuan, X. S. Wang, H. C. Zhou, *J. Am. Chem. Soc.* **2009**, *131*, 6445–6451.

[9] Crystal data for **SNU-80a**: $Cu_4C_{116.5}H_{188}N_8O_{23.5}$, $M_r = 2330.91$, tetragonal, space group $P4_2/nnm$, $a = 24.8076(3)$ Å, $c = 12.2233(2)$ Å, $V = 7522.43(18)$ Å^3, $Z = 2$, $\rho_{calcd} = 1.029$ g cm^{-3}, $\mu = 0.614$ mm^{-1}, $\lambda = 0.71073$ Å, $T = 293(2)$ K, $2\theta = 48.26°$, 215 parameters, $R_1 = 0.0761$ ($I > 2\sigma(I)$, 1810 reflections), $wR_2 = 0.2242$ (all data, 3084 reflections), GOF = 1.082. CCDC 842625 contains the supplementary crystallographic data for this paper. These data can be obtained free of charge from The Cambridge Crystallographic Data Centre via www.ccdc.cam.ac.uk/data_request/cif.

[10] S. S. Y. Chui, S. M. F. Lo, J. P. H. Charmant, A. G. Orpen, I. D. Williams, *Science* **1999**, *283*, 1148–1150.

[11] A. L. Spek, *J. Appl. Crystallogr.* **2003**, *36*, 7–13.

[12] *Materials Studio v5.5*, Accelrys Inc., San Diego, CA, **2010**.

[13] a) A. P. Nelson, O. K. Farha, K. L. Mulfort, J. T. Hupp, *J. Am. Chem. Soc.* **2009**, *131*, 458–460; b) T. K. Kim, M. P. Suh, *Chem. Commun.* **2011**, *47*, 4258–4260.

[14] a) F. Salles, G. Maurin, C. Serre, P. L. Llewellyn, C. Knofel, H. J. Choi, Y. Filinchuk, L. Oliviero, A. Vimont, J. R. Long, G. Férey, *J. Am. Chem. Soc.* **2010**, *132*, 13782–13788; b) D. Tanaka, K. Nakagawa, M. Higuchi, S. Horike, Y. Kubota, L. C. Kobayashi, M. Takata, S. Kitagawa, *Angew. Chem.* **2008**, *120*, 3978–3982; *Angew. Chem. Int. Ed.* **2008**, *47*, 3914–3918; c) H. J. Park, M. P. Suh, *Chem. Commun.* **2010**, *46*, 610–612.

[15] J. L. C. Rowsell, O. M. Yaghi, *J. Am. Chem. Soc.* **2006**, *128*, 1304–1315.

[16] a) J. P. Zhang, X. M. Chen, *J. Am. Chem. Soc.* **2008**, *130*, 6010–6017; b) R. P. Lively, M. E. Dose, J. A. Thompson, B. A. McCool, R. R. Chance, W. J. Koros, *Chem. Commun.* **2011**, *47*, 8667–8669.

[17] a) P. Küsgens, M. Rose, I. Senkovska, H. Frode, A. Henschel, S. Siegle, S. Kaskel, *Microporous Mesoporous Mater.* **2009**, *120*, 325–330; b) A. Comotti, S. Bracco, P. Sozzani, S. Horike, R. Matsuda, J. Chen, M. Takata, Y. Kubota, S. Kitagawa, *J. Am. Chem. Soc.* **2008**, *130*, 13664–13672; c) T. Ohba, H. Kanoh, K. Kaneko, *J. Phys. Chem. B* **2004**, *108*, 14964–14969; d) J. P. Zhang, A. X. Zhu, R. B. Lin, X. L. Qi, X. M. Chen, *Adv. Mater.* **2011**, *23*, 1268–1271.

[18] U. S. Raghavender, S. Aravinda, N. Shamala, Kantharaju, R. Rai, P. Balaram, *J. Am. Chem. Soc.* **2009**, *131*, 15130–15132.

[19] S. Paranthaman, F.-X. Coudert, A. H. Fuchs, *Phys. Chem. Chem. Phys.* **2010**, *12*, 8123–8129.

Received: October 1, 2011
Published online: November 3, 2011

